Received: 1 May 2023 | *Revised: 29 June 2023* | *Accepted: 29 June 2023*
DOI: 10.37917/ijeee.20.1.16 *Vol. 20 | Issue 1 | June 2024*

Iraqi Journal for Electrical and Electronic Engineering
Original Article

Open Access
IJEEE University of Basrah College of Engineering

On the Performance of Wireless-Powered NOMA Communication Networks

Noor K. Breesam*[1], Walid A. Al-Hussaibi[1], Falah H. Ali[2]
[1]Dept. of Electrical Engineering Techniques, BETC, Southern Technical University, Basrah, 42001, Iraq
[2]Communications Research Group, University of Sussex, Brighton, BN19QT, UK

Correspondance
*Noor K. Breesam
Dept. of Electrical Engineering Techniques,
BETC, Southern Technical University,
Basrah, 42001, Iraq
Email: n.k.alwaeily@fgs.stu.edu.iq

Abstract
In different modern and future wireless communication networks, a large number of low-power user equipment (UE) devices like Internet of Things, sensor terminals, and smart modules have to be supported over constrained power and bandwidth resources. Therefore, wireless-powered communication (WPC) is considered a promising technology for varied applications in which the energy harvesting (EH) from radio frequency radiations is exploited for data transmission. This requires efficient resource allocation schemes to optimize the performance of WPC and prolong the network lifetime. In this paper, harvest-then-transmit-based WP non-orthogonal multiple access (WP-NOMA) system is designed with time-split (TS) and power control (PC) allocation strategies. To evaluate the network performance, the sum rate and UEs' rates expressions are derived considering power-domain NOMA with successive interference cancellation detection. For comparison purposes, the rate performance of the conventional WP orthogonal multiple access (WP-OMA) is derived also considering orthogonal frequency-division multiple access and time-division multiple access schemes. Intensive investigations are conducted to obtain the best TS and PC resource parameters that enable maximum EH for higher data transmission rates compared with the reference WP-OMA techniques. The achieved outcomes demonstrate the effectiveness of designed resource allocation approaches in terms of the realized sum rate, UE's rate, rate region, and fairness without distressing the restricted power of far UEs.

Keywords
Wireless-powered communications; NOMA; resource allocation; energy harvesting; rate capacity.

I. Introduction

The number of wireless connected user equipments (UEs) like Internet of Things (IoT) devices and sensor nodes is expected to be enlarged in a large scale to maintain a smart lifestyle in diverse industrial, commercial, health, and security sectors. To accomplish this vital target, intensive research efforts have been steered to address the key issues in this field like massive connectivity, low energy consumption, higher data rates, wider coverage, user-fairness, robust multiple access (MA), and realistic complexity [1–6]. The UEs in diverse wireless systems such as IoT and sensor networks are typically battery-powered with limited energy. Therefore, energy harvesting (EH) based on the emitted radio frequency (RF) signals is considered as an effective solution for the sustainable (green) far-field wireless-powered communication (WPC) with near-perpetual operation [3]. The supported UEs can exploit the embedded rectennas (RF to direct current rectifiers) for charging their implemented batteries [7–9]. However, efficient resource allocation must be fulfilled for WPC systems functioning over limited power and spectrum resources [1, 5, 10, 11].

For WPC, the hybrid implementation of multiple-input multiple-output (MIMO) [12–15] and non-orthogonal MA (NOMA) [16–20] technologies can further support higher

number of UEs and transmission rates [2, 5, 6]. In power-domain NOMA, different power levels can be allocated for the connected UEs ($2 \sim 3$ in feasible systems) based on the channel gains [18]. In the uplink (UL) channel, weak UEs can utilize low power to prolong the lifetime of their embedded batteries while realizing the minimum rate request. This sustains the critical power difference with the strong UEs for effective successive interference cancellation (SIC) [18, 21].

In the literature, the important topic of RF-based WPC schemes has been examined by employing different time-split (TS) and/or power-control (PC) methodologies [1–5, 8, 10, 11, 22–28]. The optimization problem of resource management for simultaneous wireless information and power transfer (SWIPT) has been examined to maximize the energy efficiency of varied networks like IoT [3] with integrated MIMO [2] and NOMA [4]. It has been considered also for heterogeneous and cognitive radio systems [10, 22, 23]. The practical harvest-then-transmit (HtT) protocol has been employed in WPCs where the time frame is divided into two segments using TS parameter [8, 11, 26, 27]. In this protocol, the base station (BS) performs downlink (DL) phase for EH at the UEs which can be exploited for UL data transmission (DT) at the second phase. In [8, 11], and [26], NOMA has been utilized for WPC system of single-antenna BS and UE devices. The tradeoff between achieved sum rate of WPC network and user-fairness has been exposed in [11, 24], and [25].

In this research work, the performance of wireless-powered NOMA (WP-NOMA) system with SIC-based decoding is investigated by adopting HtT protocol of TS and PC resource parameters. Using BS with multiple antennas, it aims to optimize the achieved rate and EH with desired fairness of maximum sum rate and support of the minimum UEs' rates targets [9, 24]. The later issue is very important in mitigating the doubly near-far problem in WPCs since far UEs from the BS may realize lower EH but impose extra power for sum rate extension [1, 5]. The system design of WP-NOMA is described including the time frame arrangement, energy transmission (ET) model for DL, and DT model for UL channel. The TS parameter is used for the considered time frame to control the DL and UL phases while PC coefficients are used for the supported UEs. For efficient performance evaluation, the sum rate and UEs' rates are derived for WP-NOMA design and also the existing references of WP-orthogonal MA (WP-OMA) based on orthogonal frequency-division MA (OFDMA) and time-division MA (TDMA) [9, 22]. Intensive investigations are conducted to obtain the best TS and PC resource parameters that enable maximum EH for higher DT rates compared with the reference techniques. The achieved results demonstrate the effectiveness of designed resource allocation approaches in terms of the realized sum rate, UE's rate, rate region, and fairness.

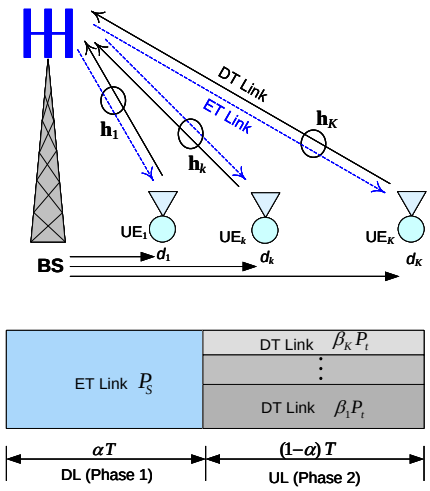

Fig. 1. The considered WP-NOMA network: (a) system design; (b) the adopted communication time frame structure.

The rest of this paper is organized as follows. Section II describes the system design of WP-NOMA. The rate analysis is presented in Section III while the simulation results are shown in Section IV. Finally, Section V concludes the work.

Notations: Uppercase and lowercase letters with bold-face stand for matrices and vectors, respectively. Plain lowercase letters stand for scalars. $\mathcal{C}^{M\times N}$ denotes complex $M \times N$ matrix. The superscripts $[.]^*$, $[.]^{\mathrm{H}}$, and $[.]^{\mathrm{T}}$ stand for complex conjugate, conjugate transposition, and transposition, respectively while $\mathbb{E}[.]$ denotes the expectation operator. I_M denotes $M \times M$ identity matrix. $\|.\|$ stands for the Euclidean vector norm while $|.|$ denotes the determinant for matrices and magnitude for vectors.

II. System Design and Modeling

This research work considers a WP-NOMA system of M-antenna BS unit communicating simultaneously over normalized bandwidth $(W = 1)$ with K single-antenna UEs as in Fig. 1. The UEs $\{\mathrm{UE}_k\}_{k=1}^{K}$ are located at fixed distances from the BS and assumed to be sorted in ascending order as $d_1 < \cdots < d_K$. The adopted HtT policy for each time frame divides the duration period (T) into two phases for ET and DT through TS parameter (α) where $0 < \alpha < 1$. A segment αT from the time frame is used in the DL for wireless ET with average power P_s. The other part $\rho T = (1-\alpha)T$ is utilized for UL channel to perform DT with total received power limit at the BS as P_t. In this configuration, the UEs exploits their EH from phase 1 to accomplish DT in the UL channel with PC parameters $\{0 < \beta_k < 1\}_{k=1}^{K}$ where $\sum_{k=1}^{K} \beta_k = 1$.

For the communication time frame, the UEs' channels

$\mathbf{h}_k = [h_{1k} \dots h_{Mk}]^T \in \mathcal{C}^{M\times 1}; \forall k$ are assumed to be perfectly available at the BS receiver, where h_{mk} stands for the channel coefficient between UE$_k$ and m^{th} receive antenna based on path loss and small-scale fading. The channel model of UE$_k$ can be represented as [6, 25]

$$\mathbf{h}_k = (\mathcal{L}_k)^{1/2} \psi_k; \forall k \tag{1}$$

where $\psi_k = [\psi_{1k} \dots \psi_{Mk}]^T \in \mathcal{C}^{M\times 1}$ denotes the channel vector whose complex Gaussian entries ψ_{mk} are belongs to flat Rayleigh fading process with zero-mean and unit-variance. The parameter $\mathcal{L}_k = d_k^{-\vartheta}$ stands for the large-scale path loss of k^{th} UE based on d_k and path loss exponent ϑ.

The EH by k^{th} UE can be found based on the ET model represented by [8]

$$E_k = \mu_k \parallel \mathbf{h}_k \parallel^2 P_s(\alpha T) \tag{2}$$

where $\mu_k = G_S G_k \eta_k$ with G_S and G_k denote the directional gains of the BS and UE$_k$ antennas, respectively while η_k is the overall EH efficiency of k^{th} UE.

The received signal model $\mathbf{r} \in \mathcal{C}^{M\times 1}$ can be given by [5]

$$r = \sum_{k=1}^{K} p_k^{1/2} v_k \mathbf{h}_k + \mathbf{n} \tag{3}$$

where v_k is the transmitted signal of k^{th} UE with $\mathbb{E}\left[v_k v_k^*\right] = 1$, and $\mathbf{n} = [n_1 \dots n_M]^T \in \mathcal{C}^{M\times 1}$ is the additive white Gaussian noise (AWGN) vector with elements of zero-mean and variance σ_n^2. For efficient SIC and inter-user interference management, sufficient power difference between the UEs' received signals of powers $\mathcal{P}_k; \forall k$ can be attained through allowed transmit power condition $p_k = \beta_k P_t / \mathcal{L}_k; \forall k$.

III. Rate Analysis

1) Rate Analysis of WP-NOMA

For the designed WP-NOMA, the sum rate can be given in terms of the UEs' rates $R_k; \forall k$ as $R_{sum}^{WP-NOMA} = \sum_{k=1}^{K} R_k$ where $R_k \geqslant R_0; \forall k$ with R_0 as the minimum rate request [5]. Therefore, for each channel realization, the sum rate of signal model (3) can be given based on UEs' powers $p_k; \forall k$ and PC parameters $\beta_k; \forall k$ as [5]

$$R_{sum}^{WP-NOMA} \leqslant \rho T \log_2 \left| \mathbf{I}_M + \gamma \sum_{k=1}^{K} \frac{\beta_k \mathbf{h}_k \mathbf{h}_k^{\mathrm{H}}}{\mathcal{L}_k} \right| \tag{4}$$

where $\gamma = P_t / \sigma_n^2$ denotes the average signal-to-noise (SNR) ratio at each of the BS antennas based on the constrained total received power (P_t) from all connected UEs and receiver noise power (σ_n^2).

Based on [5] and for each communication time frame, the rate of UE$_k; k = 1, \dots, K-1$ can be found for SIC with fixed signal decoding order from UE$_1$ to UE$_K$ as

$$R_k \leqslant \rho T \log_2 \left| \mathbf{I}_M + \frac{(\gamma \beta_k / \mathcal{L}_k) \mathbf{h}_k \mathbf{h}_k^{\mathrm{H}}}{\mathbf{I}_M + \gamma \sum_{i=k+1}^{K} \frac{\beta_i}{\mathcal{L}_i} \mathbf{h}_i \mathbf{h}_i^{\mathrm{H}}} \right|. \tag{5}$$

At the last SIC stage, the rate of UE$_K$ can be found without inter-user interference can be found as

$$R_K \leqslant \rho T \log_2 \left| \mathbf{I}_M + \gamma \frac{\beta_K \mathbf{h}_K \mathbf{h}_K^{\mathrm{H}}}{\mathcal{L}_K} \right|. \tag{6}$$

The average performance of sum rate and UEs' rates for WP-NOMA over random fading channels can be given by the mean $\mathbb{E}\left[R_{sum}^{WP-NOMA}\right]$ and $\mathbb{E}[R_k]; \forall k$, respectvely.

2) Rate Analysis of WP-OMA

For the reference WP-OMA, the UEs perform simultaneous DT in the UL over orthogonal frequency or time sub-channels with equal received power control $\mathcal{P}_k = P_t / K; \forall k$ through allocated powers $p_k = P_t / (K \mathcal{L}_k); \forall k$. Unfortunately, this will cause a *double near-far* problem [5].

For OFDMA, the UEs are assigned orthogonal frequency sub-channels of bandwidth $W_k; \forall k$. The sum rate over total system bandwidth $W = \sum_{k=1}^{K} W_K$ can be found then as [5]

$$R_{sum}^{WP-OFDMA} = \rho T \sum_{k=1}^{K} W_k \log_2 \left| \mathbf{I}_M + \frac{\gamma \mathbf{h}_k \mathbf{h}_k^{\mathrm{H}}}{W \mathcal{L}_k} \right|. \tag{7}$$

The average sum rate can be given then by $\mathbb{E}\left[R_{sum}^{WP-OFDMA}\right]$ where R_k depends on the bandwidth (W_k).

On the other hand when TDMA scheme is utilized for WP-OMA, the UEs are assigned orthogonal time sub-channels ($T_k; \forall k$) within the allocated segment of time frame in the second phase with $\sum_{k=1}^{K} T_k = \rho T$. So, the sum rate for can be found as [5]

$$R_{sum}^{WP-TDMA} = \rho T \sum_{k=1}^{K} T_k \log_2 \left| \mathbf{I}_M + \frac{\gamma \mathbf{h}_k \mathbf{h}_k^{\mathrm{H}}}{K \mathcal{L}_k} \right|. \tag{8}$$

The average sum rate can be given then as $\mathbb{E}\left[R_{sum}^{WP-TDMA}\right]$ where R_k is linearly proportional with the allowed time (T_k).

Note that for the considered WP-OMA schemes, equal UEs' rates can be achieved when equal sub-channel arrangement is employed.

IV. Simulation Results

Numerical simulations are conducted in this section using MATLAB environment to demonstrate the performance of WP-NOMA system. The achieved results of sum rate, UE's

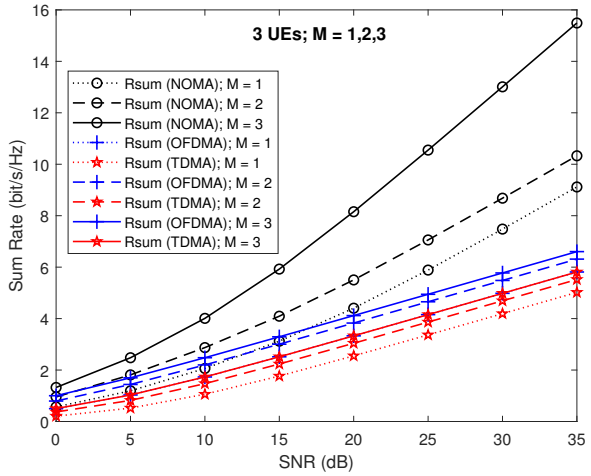

Fig. 2. The sum rate of 3 UEs WP-NOMA as a function of SNR compared with the references where $M = 1, 2$, and 3, $\alpha = 0.5$, $\beta_1 = 0.7$, $\beta_2 = 0.2$, and $\beta_3 = 0.1$, $d_1 = 50$ m, $d_2 = 55$ m, and $d_3 = 65$ m.

rate, rate region, and EH are averaged over 10^4 channel realizations. The outcomes are utilized to obtain the best TS and PC parameters that enable maximum EH for higher DT rates with user-fairness and energy saving of far UEs. The realized rate outcomes (bit/s/Hz) and EH (Joule) are compared with reference WP-OMA that employ OFDMA or TDMA techniques of equal sub-channel divisions. The considered simulation parameters are: $K = 2$ and 3 UEs located at fixed distances d_k; $\forall k$ in meter; $M = 1 \rightarrow 3$; $P_s = K$; $P_t = 1$; $\mu_k = 1$; $\forall k$; $T = W = 1$; $\vartheta = 3.8$; and $R_0 = 0.1$ bit/s/Hz.

1) Rate Results

In Fig. 2, the sum rate results of 3 UEs WP-NOMA are shown based on (4), (7), and (8) as a function of SNR where $M = 1, 2$, and 3, $\alpha = 0.5$, $\beta_1 = 0.7$, $\beta_2 = 0.2$, $\beta_3 = 0.1$, $d_1 = 50$ m, $d_2 = 55$ m, and $d_3 = 65$ m. The obtained outcomes show the superiority of designed system compared with the reference WP-OMA schemes (OFDMA and TDMA) for all SNR values and any utilized number of BS antennas (M). Furthermore, the achieved gain of sum rate is enlarged considerably as the spatial diversity (M) increased. For example when SNR of 20 dB and $M = 3$ are considered, a sum rate of 8.153 bit/s/Hz is found which significantly outperforms OFDMA and TDMA by about 4 and 4.8 bit/s/Hz, respectively. Fig. 3 (a), (b), and (c) show the realized UEs' rates of this scenario as a function of SNR using (5)-(8). For BS of $M = 2$, the rate performance depends completely on the power-domain NOMA. In this case, UE_1 show higher rate at low $\sim$ moderate SNRs, and saturated at high SNR levels. This is owing to high inter-user interference level from the other UEs compared with noise power. UE_2 and UE_3 of low and free interference values, re-

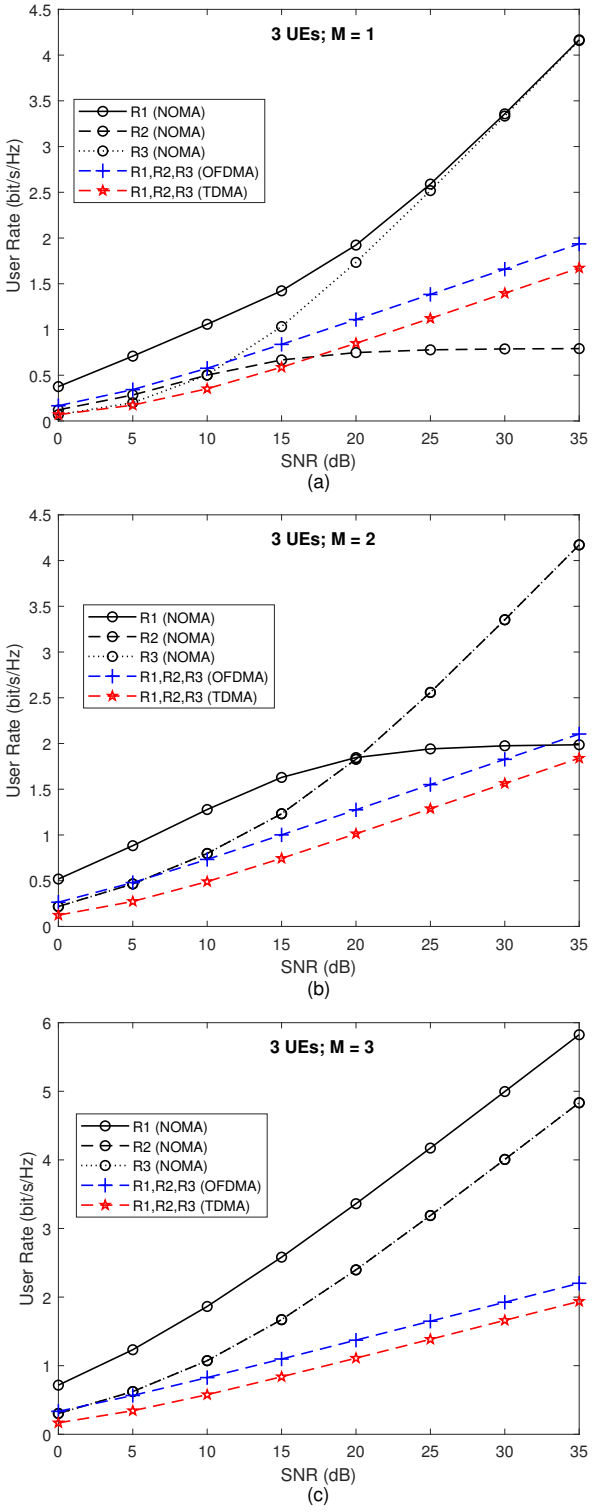

Fig. 3. The UEs' rates of 3 UEs WP-NOMA as a function of SNR compared with the references wher $M = 1, 2$, and 3, $\alpha = 0.5$, $\beta_1 = 0.7$, $\beta_2 = 0.2$, and $\beta_3 = 0.1$, $d_1 = 50$ m, $d_2 = 55$ m, and $d_3 = 65$ m.: (a) $M = 1$; (b) $M = 2$; (c) $M = 3$.

TABLE I.
SUMMARY OF RATE RESULTS OF 3 UES SYSTEM AT SNR OF 20 *dB* IN FIGS. 2 AND 3 COMPARED WITH THE REFERENCE WP-OMA SCHEMES.

M	Rate	Considered Schemes in bit/s/Hz		
		WP-NOMA	WP-OMA	
			OFDMA	TDMA
1	R_{sum}	4.292	3.324	2.547
	R_1	1.922	1.108	0.849
	R_2	0.747	1.108	0.849
	R_3	1.733	1.108	0.849
2	R_{sum}	5.502	3.826	3.046
	R_1	1.846	1.274	1.014
	R_2	1.828	1.274	1.014
	R_3	1.828	1.274	1.014
3	R_{sum}	8.153	4.116	3.327
	R_1	3.361	1.372	1.109
	R_2	2.396	1.372	1.109
	R_3	2.396	1.372	1.109

spectively demonstrate increased performances as the SNR increased. This issue has direct effect on managing the limited EH due to far distances compared with the nearest UE_1. The UEs can operate in *max-min* fairness configuration with about 1.82 bit/s/Hz at 20 dB. For $M \geq K$, all UEs can achieve proportional fairness which enlarges the sum rate. The UEs' rates are increased as the SNR increases irrespective of their actual distances from the BS and PC allocation. The baseline OFDMA and TDMA techniques of equal sub-channels achieve equal UEs' rates for all considered BS antennas. For instance when SNR of 20 dB and $M = 3$ are considered, the designed system achieves 3.361, 2.396, and 2.396 bit/s/Hz for UE_1, UE_2, and UE_3, respectively compared with 1.372 and 1.109 bit/s/Hz for UEs in OFDMA and TDMA schemes, respectively. In Table I, summary of the realized outcomes at SNR of 20 dB is given to demonstrate the tradeoffs in system performance.

In Fig. 4, the rate performance of 3 UEs WP-NOMA system is shown using (4)-(6) as a function of the distance d_1 of UE_1 in meter (m) where the other UEs' distances are used as $d_2 = d_1 + 5$ m and $d_3 = d_2 + 5$ m. The other considered parameters are BS antennas as M=1,2, and 3, TS as $\alpha = 0.5$, PC as $\beta_1 = 0.7$, $\beta_2 = 0.2$, $\beta_3 = 0.1$, and SNR of 20 dB. From the achieved outcomes, it can be seen clearly that the sum rate and UEs' rates are constant as the distances increased. This is owing to the utilized TS and PC parameters (i.e. α, β_1, β_2, and β_3). Besides, the sum rate of the designed system is increased significantly as the spatial diversity increased based on the utilized number of BS antennas (M) while the achieved UEs' rates depend on the allocated power through PC parameters.

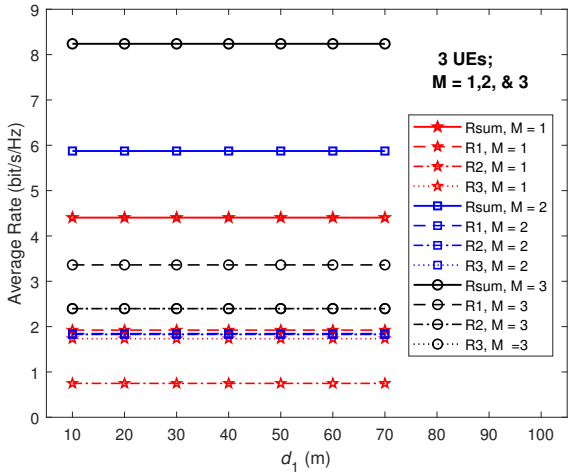

Fig. 4. The rate performance of 3 UEs WP-NOMA as a function of d_1 where $d_2 = d_1 + 5$ m, $d_3 = d_2 + 5$ m, $M = 1, 2,$ and 3, $\beta_1 = 0.7$, $\beta_2 = 0.2$, $\beta_3 = 0.1$, and SNR of 20 dB.

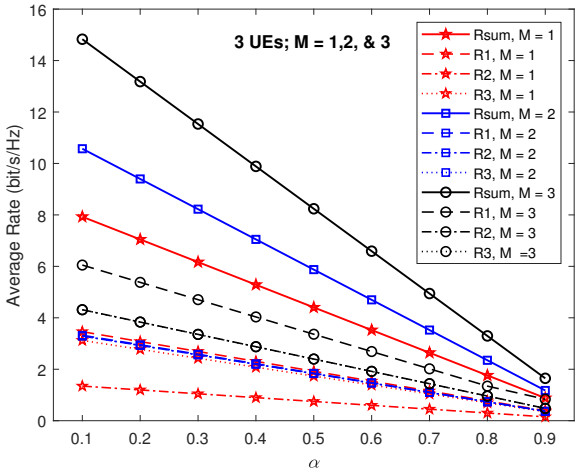

Fig. 5. The rate performance of 3 UEs WP-NOMA as a function of α where $M = 1, 2,$ and 3, $\beta_1 = 0.7$, $\beta_2 = 0.2$, $\beta_3 = 0.1$, $d_1 = 10$ m, $d_2 = 20$ m, $d_3 = 30$ m, and SNR of 20 dB.

To investigate the rate performance of WP-NOMA as a function of TS parameter (α), Fig. 5 presents the sum rate and UEs' rates ((4)-(6)) for 3 UEs system at SNR of 20 dB with $d_1 = 10$ m, $d_2 = 20$ m, $d_3 = 30$ m, $\beta_1 = 0.7$, $\beta_2 = 0.2$, and

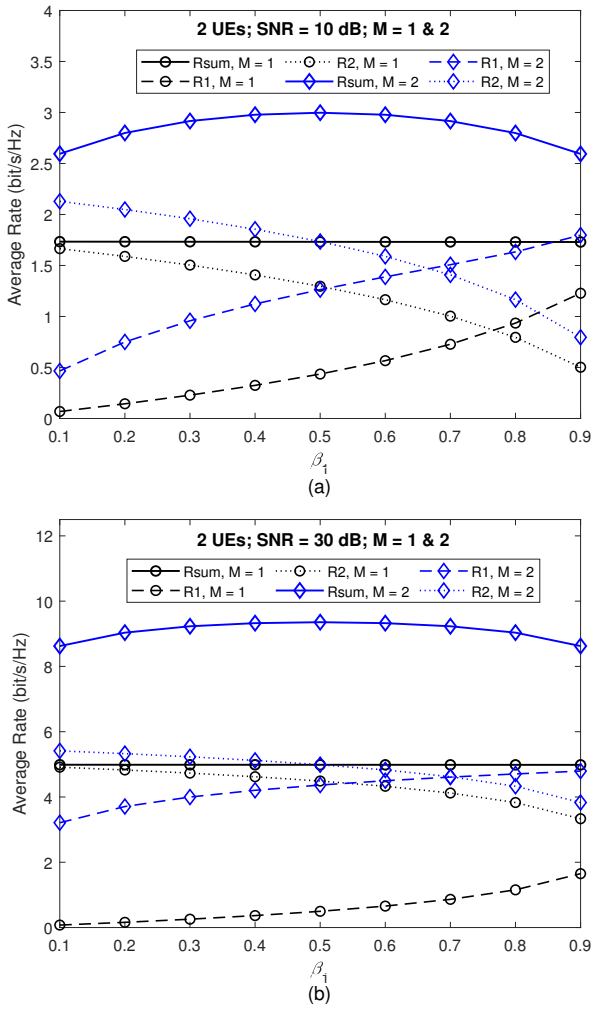

Fig. 6. The rate performance of 2 UEs WP-NOMA as a function of β_1 where $\beta_2 = 1-\beta_1$, $M = 1$ and 3, $\alpha = 0.5$, $d_1 = 20$ m, $d_2 = 40$ m : (a) SNR=10 dB; (b) SNR=30 dB.

$\beta_3 = 0.1$, $M = 1,2$,and 3. The achieved results demonstrate that the rate performance is generally decreased as α increased (i.e. inversely proportional relation) due to reduced portion of time for DT link phase. However, the amount of available energy at each UE has also direct impact on the achieved rates. This depends mainly on the EH level during the first phase of ET from the BS.

In Fig. 6 (a) and (b), the rate of 2 UEs WP-NOMA is shown using (4)-(6) as a function of PC allocation parameter β_1 with $\beta_2 = 1-\beta_1$ and for SNR of 10 dB and 30 dB, respectively. The considered system parameters are $\alpha = 0.5$, $d_1 = 20$ m, $d_2 = 40$ m, and BS antennas of $M = 1$ and 2. The realized outcomes show that the UEs' rates depend on the allocated power for DT is generally increased as the PC parameter increased (i.e. directly proportional relation) and further enhanced with increased spatial diversity (M) and/or SNR level. However, the sum rate performance is shown to be maximized at moderate levels of PC parameters (β_1 and β_2)

2) Rate Region for 2 UE Scenario

In Fig. 7 (a), (b), and (c), the rate region of 2 UEs WP-NOMA scenario ((5),(6)) is shown for SNR of 20 dB using TS parameter of $\alpha = 0.3$, 0.5, and 0.8, respectively compared with the reference WP-OMA schemes ((7),(8)). The considered system parameters are $M = 1$, $d_1 = 10$ m, $d_2 = 30$ m, and PC parameters of $\beta_1 = 0.8$ and $\beta_2 = 0.2$. Without spatial diversity ($M = 1$), the operating rate point $A = (R_1, R_2)$ at the corner of the pentagon is shown to be directly influenced with the utilized TS parameter (α). For instance, the point $A = (1.581, 3.08)$ is realized with $R_{sum} = 4.661$ bit/s/Hz when $\alpha = 0.3$ while point $A = (0.451, 0.88)$ is found with $R_{sum} = 1.331$ bit/s/Hz when $\alpha = 0.8$. Note that the obtained rate points for WP-OMA schemes based on OFDAM are placed on the face of the rate region while the point of TDMA scheme is located inside the region which demonstrates considerable performance gap compared with the designed system. In Fig. 8 (a) and (b), the spatial diversity for the considered WP-NOMA system with $\alpha = 0.5$ is increased to $M = 2$ and 3, respectively. It can be seen clearly the realized operating rate points demonstrate higher sum rate as $A = (3.075, 2.684)$ with $R_{sum} = 5.759$ bit/s/Hz when $M = 2$, and $A = (3.497, 2.968)$ with $R_{sum} = 6.465$ bit/s/Hz when $M = 3$ compared with the case of $M = 1$ which operate on the corner point $A = (1.129, 2.2)$ with $R_{sum} = 3.329$ bit/s/Hz. Besides, the rate points for both reference schemes (TDMA and OFDMA) are located inside the rate region with significant performance gap.

3) EH Results

In Fig. 9, the EH performance of 2 UEs WP-NOMA system is shown using (2) as a function of SNR where $d_1 = 10$ m, $d_2 = 30$ m, $M = 1,2$, and 3, $\alpha = 0.5$, $\beta_1 = 0.8$, and $\beta_2 = 0.2$. It can be seen that the EH level of connected UEs are constant over all SNRs owing to the employed TS and PC parameters (i.e. α, β_1, and β_2). Besides, the achieved EH by UEs are increased significantly as the spatial diversity increased based on the utilized number of BS antennas from $M = 1$ to $M = 3$ which greatly improves the emitted RF signals. For instance, UE_1 achieves EH of $E_1 = 0.79$ mJoule when $M = 1$ and increased significantly to $E_1 = 2.4$ mJoule for $M = 3$ (i.e. about threefold EH level). Summary of the realized outcomes at SNR of 20 dB is shown in Table II.

To investigate the EH performance of WP-NOMA as a function of TS parameter (α), Fig. 10 shows the outcomes using (2) for 2 UEs scenario at SNR of 20 dB with $d_1 = 20$ m,

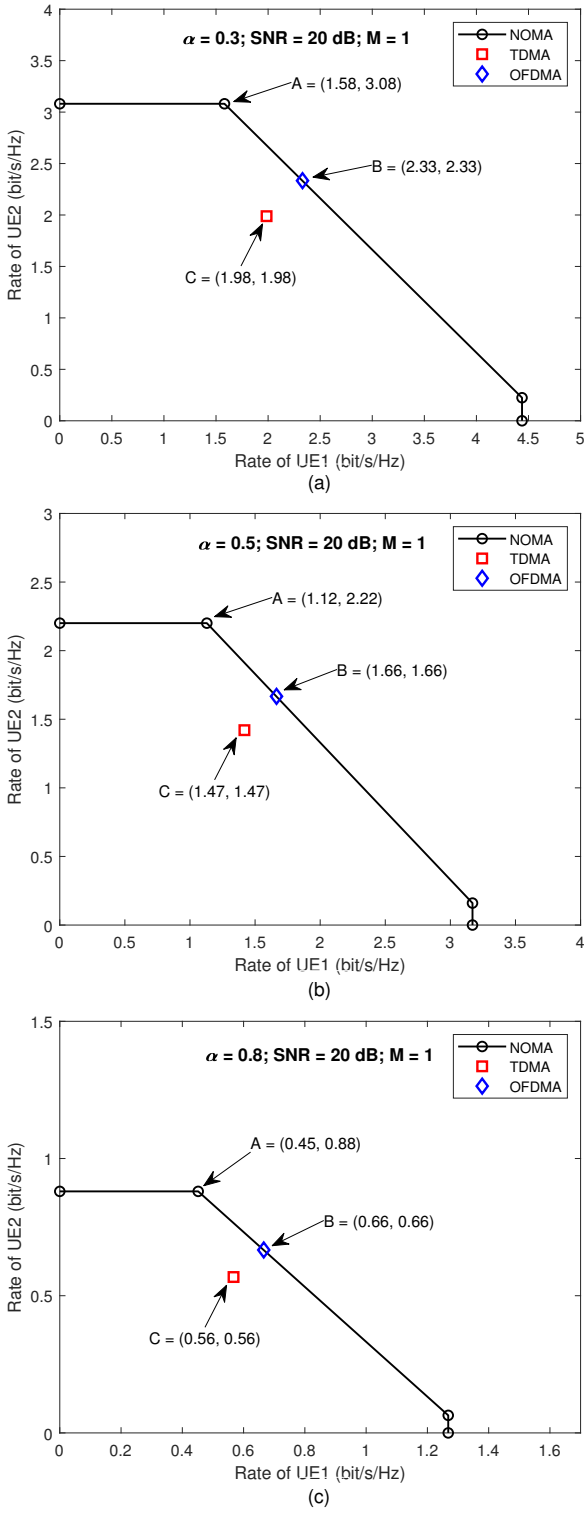

Fig. 7. The rate region of 2 UEs WP-NOMA with the references where $M = 1$, $d_1 = 10$ m, $d_2 = 30$ m, $\beta_1 = 0.8$, $\beta_2 = 0.2$, and SNR of 20 dB: (a) $\alpha = 0.3$; (b) $\alpha = 0.5$; (c) $\alpha = 0.8$.

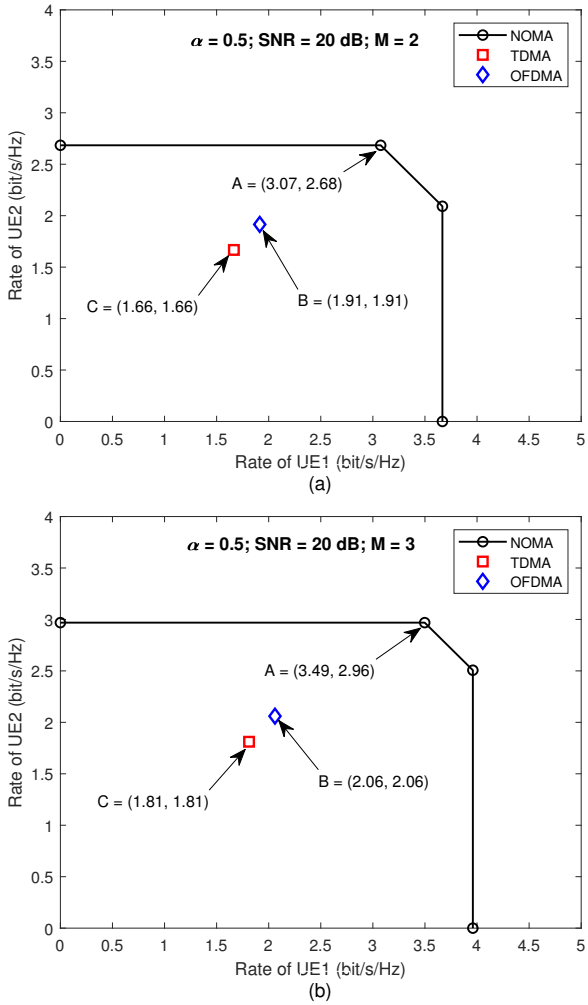

Fig. 8. The rate region of 2 UEs WP-NOMA with the references where $\alpha = 0.5$, $d_1 = 10$ m, $d_2 = 30$ m, $\beta_1 = 0.8$, $\beta_2 = 0.2$, and SNR of 20 dB : (a) $M = 2$; (b) $M = 3$.

$d_2 = 70$ m, $\beta_1 = 0.8$, $\beta_2 = 0.2$, $M = 1, 2$, and 3. The achieved results demonstrate that the EH performance is generally increased as α increased as expected owing to increased portion of time for ET link. Additionally, the achieved EH levels by UEs are increased significantly as the spatial diversity increased based on the utilized number of BS antennas from $M = 1$ to $M = 3$. In Fig. 11, the EH performance (2) of 2 UEs system is shown as a function of d_1 where $d_2 = d_1 + 5$ m. The other considered parameters are BS antennas of $M = 1, 2$, and 3, TS as $\alpha = 0.5$, PC as $\beta_1 = 0.8$ and $\beta_2 = 0.2$, and SNR of 20 dB. It can be seen that the UEs' EH performances are decreased as the distances increased due to the utilized TS and path loss parameters irrespective of the constructive impact of spatial diversity.

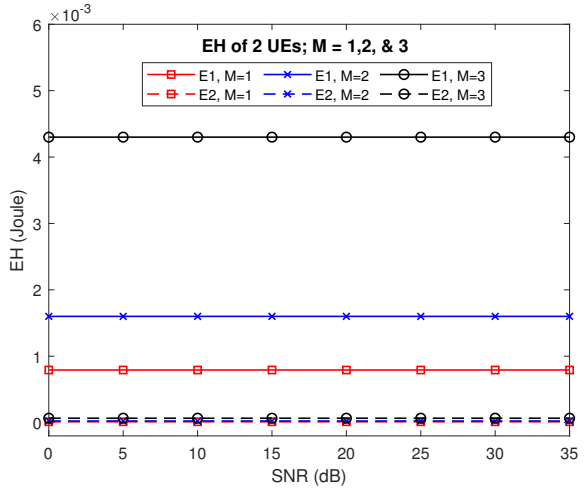

Fig. 9. The energy harvested of 2 UEs WP-NOMA as a function of SNR where $d_1 = 10$ m, $d_2 = 30$ m, $M = 1,2$, and 3, $\alpha = 0.5$, $\beta_1 = 0.8$ and $\beta_2 = 0.2$.

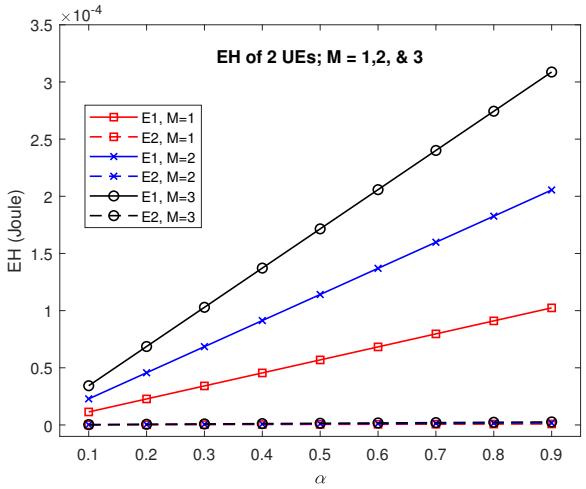

Fig. 10. The energy harvested of 2 UEs WP-NOMA as a function of α where $d_1 = 20$ m, $d_2 = 70$ m, $M = 1,2$, and 3, $\beta_1 = 0.8$, $\beta_2 = 0.2$, and SNR of 20 dB.

V. Conclusions

In this work, HtT-based WP-NOMA has been examined to improve the network performance in terms of sum rate, UE's rate, EH level, and fairness. Through the adopted time frame configuration, the UEs accomplish EH during the DL to perform DT in the UL phase. For the UL with SIC, the sum rate and UEs' rates expressions have been derived considering the key parameters for TS and PC allocation. The outcomes have shown that the sum rate performs directly with SNR and inversely with the TS parameter and UE distance. On the other hand, the UEs' rates depend directly on TS and the allocated power through PC parameters, and inversely with the UE distance. The achieved EH level is directly affected by the TS parameter and inversely with the UE distance. The spatial diversity of BS antennas has positive impact on enhancing the performance. The achieved results validated the effectiveness of designed WP-NOMA networks compared with reference schemes. By proper selection of TS and PC parameters, significant increase in sum rate, UE's rate, and EH can be realized with valuable tradeoffs in desired user-fairness. This has direct impact on mitigating the double near-far challenge towards near-perpetual network operation.

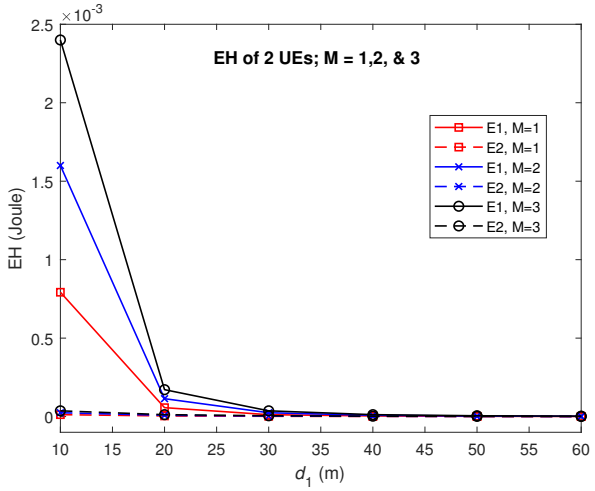

Fig. 11. The energy harvested of 2 UEs WP-NOMA as a function of d_1 where $d_2 = d_1 + 20$ m, $M = 1,2$, and 3, $\beta_1 = 0.8$, $\beta_2 = 0.2$, and SNR of 20 dB.

TABLE II.
SUMMARY OF OF THE EH RESULTS OF 2 UES WP-NOMA AT SNR OF 20 *dB* WHERE THE SYSTEM PARAMETERS AS: $d_1 = 10\ m$, $d_2 = 30\ m$, $\alpha = 0.5$, $\beta_1 = 0.8$, AND $\beta_2 = 0.2$.

BS Antennas	Energy Measure	EH Results (Joule)
$M = 1$	E_1	0.79×10^{-3}
	E_2	0.012×10^{-3}
$M = 2$	E_1	1.6×10^{-3}
	E_2	0.024×10^{-3}
$M = 3$	E_1	2.4×10^{-3}
	E_2	0.036×10^{-3}

Conflict of Interest

The authors have no conflict of relevant interest to this article.

REFERENCES

[1] Y. Cheng, K. H. Li, K. C. Teh, S. Luo, and B. Li, "Two-tier noma-based wireless powered communication networks," *IEEE Systems Journal*, vol. 16, no. 3, pp. 4698–4707, 2021.

[2] G. Femenias, J. García-Morales, and F. Riera-Palou, "Swipt-enhanced cell-free massive mimo networks," *IEEE Transactions on Communications*, vol. 69, no. 8, pp. 5593–5607, 2021.

[3] L. Chen, B. Hu, G. Xu, and S. Chen, "Energy-efficient power allocation and splitting for mmwave beamspace mimo-noma with swipt," *IEEE Sensors Journal*, vol. 21, no. 14, pp. 16381–16394, 2021.

[4] H. Yang, Y. Ye, X. Chu, and M. Dong, "Resource and power allocation in swipt-enabled device-to-device communications based on a nonlinear energy harvesting model," *IEEE Internet of Things Journal*, vol. 7, no. 11, pp. 10813–10825, 2020.

[5] N. K. Breesam, W. A. Al-Hussaibi, F. H. Ali, and I. M. Al-Musawi, "Efficient resource allocation for wireless-powered mimo-noma communications," *IEEE Access*, vol. 10, pp. 130302–130313, 2022.

[6] W. A. Al-Hussaibi and F. H. Ali, "Efficient user clustering, receive antenna selection, and power allocation algorithms for massive mimo-noma systems," *IEEE Access*, vol. 7, pp. 31865–31882, 2019.

[7] J. Hu, K. Yang, G. Wen, and L. Hanzo, "Integrated data and energy communication network: A comprehensive survey," *IEEE Communications Surveys & Tutorials*, vol. 20, no. 4, pp. 3169–3219, 2018.

[8] P. D. Diamantoulakis, K. N. Pappi, Z. Ding, and G. K. Karagiannidis, "Wireless-powered communications with non-orthogonal multiple access," *IEEE Transactions on Wireless Communications*, vol. 15, no. 12, pp. 8422–8436, 2016.

[9] S. Kashyap, E. Björnson, and E. G. Larsson, "On the feasibility of wireless energy transfer using massive antenna arrays," *IEEE Transactions on Wireless Communications*, vol. 15, no. 5, pp. 3466–3480, 2016.

[10] H. Zhang, M. Feng, K. Long, G. K. Karagiannidis, V. C. Leung, and H. V. Poor, "Energy efficient resource management in swipt enabled heterogeneous networks with noma," *IEEE Transactions on Wireless Communications*, vol. 19, no. 2, pp. 835–845, 2019.

[11] P. D. Diamantoulakis and G. K. Karagiannidis, "Maximizing proportional fairness in wireless powered communications," *IEEE Wireless Communications Letters*, vol. 6, no. 2, pp. 202–205, 2017.

[12] A. Goldsmith, S. A. Jafar, N. Jindal, and S. Vishwanath, "Capacity limits of mimo channels," *IEEE Journal on selected areas in Communications*, vol. 21, no. 5, pp. 684–702, 2003.

[13] Y. Gao, H. Vinck, and T. Kaiser, "Massive mimo antenna selection: Switching architectures, capacity bounds, and optimal antenna selection algorithms," *IEEE Transactions on signal processing*, vol. 66, no. 5, pp. 1346–1360, 2017.

[14] W. A. Al-Hussaibi and F. H. Ali, "A closed-form approximation of correlated multiuser mimo ergodic capacity with antenna selection and imperfect channel estimation," *IEEE Transactions on vehicular technology*, vol. 67, no. 6, pp. 5515–5519, 2018.

[15] W. A. Al-Hussaibi and F. H. Ali, "Performance-complexity tradeoffs of mimo-noma receivers towards green wireless networks," in *2019 IEEE 30th annual international symposium on personal, indoor and mobile radio communications (PIMRC)*, pp. 1–6, IEEE, 2019.

[16] L. Dai, B. Wang, Z. Ding, Z. Wang, S. Chen, and L. Hanzo, "A survey of non-orthogonal multiple access for 5g," *IEEE communications surveys & tutorials*, vol. 20, no. 3, pp. 2294–2323, 2018.

[17] B. Makki, K. Chitti, A. Behravan, and M.-S. Alouini, "A survey of noma: Current status and open research challenges," *IEEE Open Journal of the Communications Society*, vol. 1, pp. 179–189, 2020.

[18] S. R. Islam, N. Avazov, O. A. Dobre, and K.-S. Kwak, "Power-domain non-orthogonal multiple access (noma) in 5g systems: Potentials and challenges," *IEEE Communications Surveys & Tutorials*, vol. 19, no. 2, pp. 721–742, 2016.

[19] W. Al-Hussaibi, "Optimal cluster formation and power control for high connectivity wireless mimo-noma applications," *Electronics Letters*, vol. 55, no. 20, pp. 1110–1112, 2019.

[20] I. Al-Musawi, W. Al-Hussaibi, and F. Ali, "Chaos-based physical layer security in noma networks over rician fading channels," in *2021 IEEE International Conference on Communications Workshops (ICC Workshops)*, pp. 1–6, IEEE, 2021.

[21] I. M. Al-Musawi, W. A. Al-Hussaibi, and F. H. Ali, "Efficient secure noma schemes based on chaotic physical layer security for wireless networks," *IEEE Open Journal of the Communications Society*, vol. 3, pp. 2425–2443, 2022.

[22] T. A. Khan, A. Yazdan, and R. W. Heath, "Optimization of power transfer efficiency and energy efficiency for wireless-powered systems with massive mimo," *IEEE Transactions on Wireless Communications*, vol. 17, no. 11, pp. 7159–7172, 2018.

[23] D. Xu and Q. Li, "Joint power control and time allocation for wireless powered underlay cognitive radio networks," *IEEE Wireless Communications Letters*, vol. 6, no. 3, pp. 294–297, 2017.

[24] J. Tang, Y. Yu, M. Liu, D. K. So, X. Zhang, Z. Li, and K.-K. Wong, "Joint power allocation and splitting control for swipt-enabled noma systems," *IEEE Transactions on Wireless Communications*, vol. 19, no. 1, pp. 120–133, 2019.

[25] T.-V. Nguyen, V.-D. Nguyen, D. B. da Costa, and B. An, "Hybrid user pairing for spectral and energy efficiencies in multiuser miso-noma networks with swipt," *IEEE Transactions on Communications*, vol. 68, no. 8, pp. 4874–4890, 2020.

[26] C. Guo, B. Liao, L. Huang, Q. Li, and X. Lin, "Convexity of fairness-aware resource allocation in wireless powered communication networks," *IEEE Communications Letters*, vol. 20, no. 3, pp. 474–477, 2016.

[27] S. K. Zaidi, S. F. Hasan, and X. Gui, "Evaluating the ergodic rate in swipt-aided hybrid noma," *IEEE Communications Letters*, vol. 22, no. 9, pp. 1870–1873, 2018.

[28] Z. Wei, X. Yu, D. W. K. Ng, and R. Schober, "Resource allocation for simultaneous wireless information and power transfer systems: A tutorial overview," *Proceedings of the IEEE*, vol. 110, no. 1, pp. 127–149, 2021.